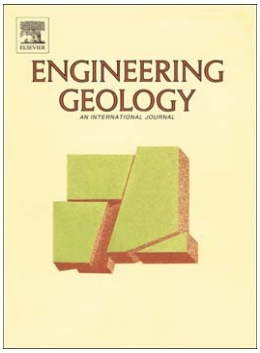

Multi-technique approach to rockfall monitoring in the Montserrat massif (Catalonia, NE Spain)

M. Janeras, J.A. Jara, M.J. Royán, J.M. Vilaplana, A. Aguasca, X. Fàbregas, J.A. Gili, P. Buxó

PII: S0013-7952(16)30851-1
DOI: doi:10.1016/j.enggeo.2016.12.010
Reference: ENGEO 4440

To appear in: *Engineering Geology*

Received date: 19 April 2016
Revised date: 15 December 2016
Accepted date: 21 December 2016

Please cite this article as: Janeras, M., Jara, J.A., Royán, M.J., Vilaplana, J.M., Aguasca, A., Fàbregas, X., Gili, J.A., Buxó, P., Multi-technique approach to rockfall monitoring in the Montserrat massif (Catalonia, NE Spain), *Engineering Geology* (2016), doi:10.1016/j.enggeo.2016.12.010

Multi-technique approach to rockfall monitoring in the Montserrat Massif (Catalonia, NE Spain)

M Janeras[1a], JA Jara[1b], MJ Royán[2], JM Vilaplana[2], A Aguasca[3], X Fàbregas[3], JA Gili[4], P Buxó[1a]

[1a] Geological Risk Prevention and Geotechnics Department, Geographical and Geological Survey of Catalonia (ICGC, Institut Cartogràfic i Geològic de Catalunya)
[1b] Geophysics and Seismology Department, Geographical and Geological Survey of Catalonia (ICGC, Institut Cartogràfic i Geològic de Catalunya)
[2] RISKNAT Group, GEOMODELS. Department of Earth and Ocean Dynamics, Faculty of Geology, University of Barcelona (UB)
[3] RSLAB - Research Group on Remote Sensing. Signal Theory and Communications Department, Technical University of Catalonia (UPC)
[4] Division of Geotechnical Engineering and Geosciences, Civil and Environmental Engineering Department, Technical University of Catalonia (UPC)

E-mail: marc.janeras@icgc.cat

Abstract. Montserrat Mountain is located near Barcelona in Catalonia, in the northeast of Spain, and its massif is formed by conglomerate interleaved by siltstone/sandstone with steep slopes very prone to rockfalls. The increasing number of visitors in the monastery area, reaching 2.4 million per year, has highlighted the risk derived from rockfalls for this building area and also for the terrestrial accesses, both roads and the rack railway. A risk mitigation plan has been launched, and its first phase during 2014-2016 has been focused largely on testing several monitoring techniques for their later implementation. The results of the pilot tests, performed as a development from previous sparse experiences and data, are presented together with the first insights obtained. These tests combine four monitoring techniques under different conditions of continuity in space and time domains, which are: displacement monitoring with Ground-based Synthetic Aperture Radar and characterization at slope scale, with an extremely non-uniform atmospheric phase screen due to the stepped topography and atmosphere stratification; Terrestrial Laser Scanner surveys quantifying the frequency of small or even previously unnoticed rockfalls, and monitoring rock block centimetre scale displacements; the monitoring of rock joints implemented through a wireless sensor network with an ad hoc design of ZigBee loggers developed by ICGC; and, finally, monitoring singular rock needles with Total Station.

Keywords. Monitoring, precursory displacement, rockfall, TLS, GBSAR, Wireless Sensor Network

1. Introduction

1.1. Situation and background

Montserrat Mountain is located near Barcelona in Catalonia, in the northeast of Spain (figure 1). This isolated massif formed by thick layers of conglomerate interleaved by siltstone/sandstone from a Late-Eocene fan-delta emerges over the Llobregat River with an overall height difference of 1000 m (from 200 to 1200 m.a.s.l.). This configuration leads to staggered slopes where vertical cliffs of conglomerate alternate with steep slopes of softer ground covered by densely vegetated colluvial

deposits (figure 2). The low tectonic activity affecting this massif has preserved the horizontality of the stratigraphic layers, but also conduced to the formation of a few dominant joint sets which are quite planar, vertical, orthogonal, very persistent and with spacing usually ranging from 1 to 10 m [Alsaker *et al.* 1996 and López-Blanco *et al.* 2000]. A main consequence of this geological structure is that the massif is very prone to rockfalls, including large single blocks typically up to 10^3 m^3.

Figure 1. Location map of Montserrat Mountain, 50 km NW of Barcelona in Catalonia (NE corner of Spain).

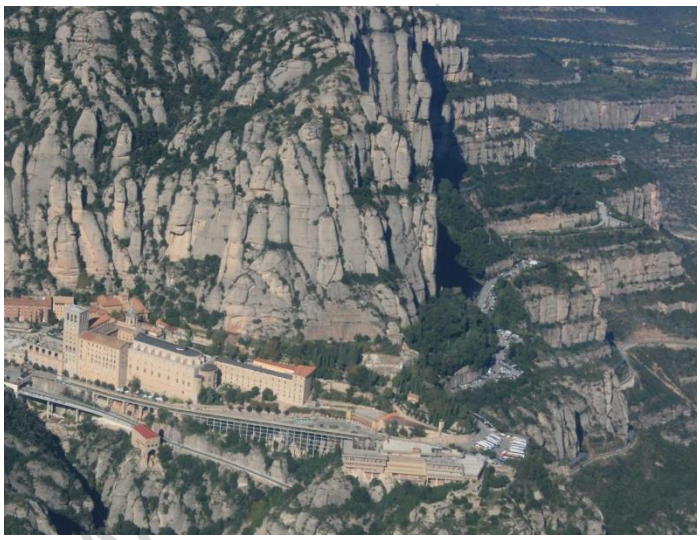

Figure 2. Overview of Montserrat Monastery area (SE edge of Montserrat Mountain). The access by road and railway can be seen at the foot of the Monastery, coming from the right bottom part of the scene, where the parking slots and the staggered slopes can be appreciated as well. All the conglomerate cliffs are potential sources of rockfalls (see the main text for additional geological description).

The Montserrat massif constitutes a Natural Park (about 3500 ha) and hosts a sanctuary and monastery with a millenarian history and great tradition in Catalonia. The monastery and some tourist premises are located at the SE edge of the mountain at 700 m.a.s.l. Combining the local and foreign tourism or pilgrimage, the number of visitors in the monastery area has been increasing yearly, reaching 2.4 million in 2014. Furthermore, nowadays it is estimated that an additional 0.8 million people per year come to the Natural Park for hiking or climbing.

The rockfall hazard, along with the concentrated exposure of visitors, highlight the risk derived from rockfalls for this building area and also for the terrestrial accesses, both roads and the rack railway [Fontquerni *et al.* 2013] and [Palau *et al.* 2011] (figure 2).

1.2. Rockfall risk

In this particular massif, rock mass instabilities range over six orders of magnitude in volume, as shown in table 1. From lower to higher volume, it starts with the disaggregation of pebbles from the conglomerate (M3); as the second group (M2) we distinguish the slabs and plates (or sheeting joints according to Hencher *et al.*, 2011) related to physical weathering; and finally, monolithic rock masses delimited by widely spaced joints with very high persistence, (M1). Several recent rockfalls have highlighted the fact that the rockfall frequency is higher than social perception tends to recognize (figure 3). After [Royán & Vilaplana 2012] and [Janeras *et al.* 2013], a frequency of about 10 rockfalls per year is estimated for magnitude over few cubic metres in the overall mountain massif.

Table 1. Summary of rockfall mechanisms and associated magnitude degree.

	Block Description	Instability Mechanism	Frequent volume	Approximate Shape
M1	Great blocks, needles and singulars masses	Stability controlled by the shear strength of discontinuities (vertical joints for lateral release and horizontal stratification at bottom and roof)	30 m^3 – 1000 m^3	prism
M2	Plates and slabs	Near-surface weathering promoting exfoliation	0.3 m^3 – 10 m^3	plate
M3	Pebbles and aggregates	Weathering the cementing matrix and shedding the pebbles from conglomerate	0.001 m^3 – 0.03 m^3	oval

Up to 2014, many active and passive protection works had been carried out, mainly along the railway and, after several major rockfalls, also along the road access [Janeras *et al.* 2011]. In 2014 a new 3-year plan for global risk mitigation was started. It is funded by the Catalan Government, promoted by Patronat de la Muntanya de Montserrat (PMM, the public entity that manages the site as a natural and cultural heritage) and executed or technically directed by Institut Cartogràfic i Geològic de Catalunya (ICGC, the public service for cartography and geology in Catalonia).

Figure 3. 28 December 2008 rockfall event of 890 m^3 at Degotalls cliff (a). In the left-hand pictures, the impacts on the road (b) and the railway (c) can be appreciated. Elevations are annotated in m.a.s.l.

For the larger rockfalls, stabilization measures are only possible in some specific cases; also passive defences, such as rockfall fences, offer only partial protection from low magnitude rockfalls. Therefore, monitoring is explored as a new line of work in Montserrat. While an early warning system (EWS) is not feasible at the present state of experience in this site, at least it will improve the knowledge on the failure triggering factors, which is a main goal of the current risk mitigation plan in the short term. The aim of this hazard control strategy is to aid in setting priorities for stabilization works, contributing to a sustainable risk management strategy.

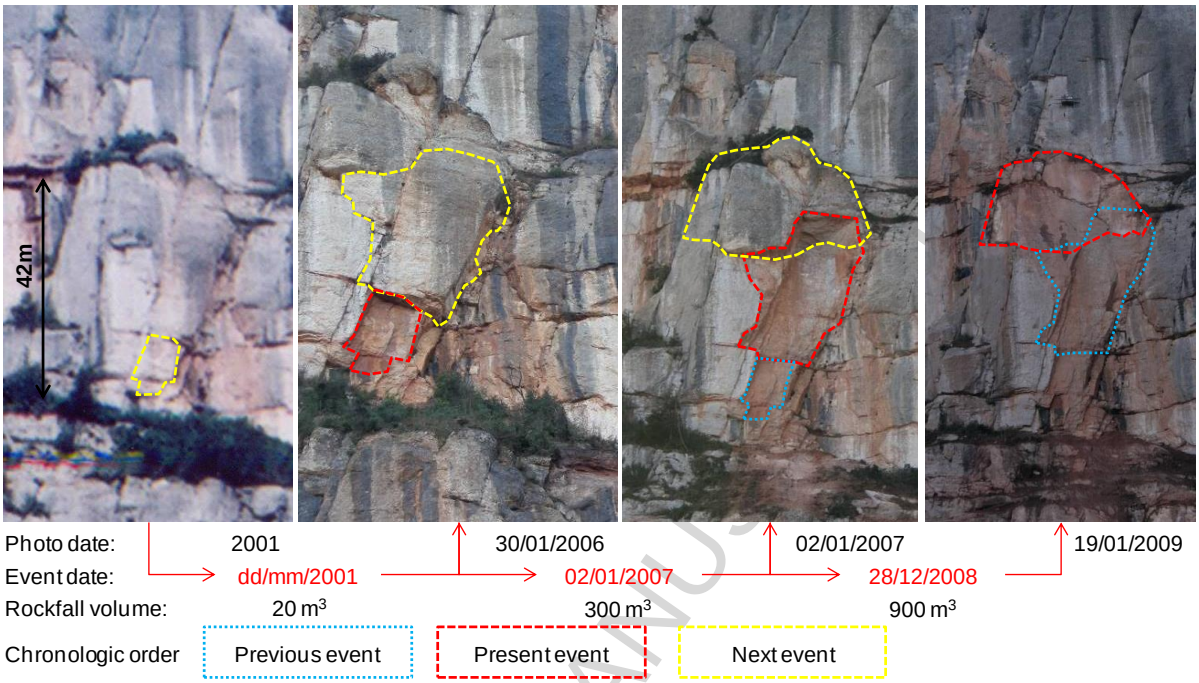

Figure 4. Successive adjacent rockfalls at the Degotalls wall corresponding to a progressive failure: a case example that drew attention to the suitability of monitoring.

In this regard, successive rockfalls detached between 2001 and 2008 from the 170m high cliff called Degotalls (figure 4) drew attention to the importance of detecting the propagation of fractures in the rock mass. Two approaches are needed: detecting partial collapses, even if they are small, that could reveal larger failure preparation, and detecting deformation on the rock wall during the rupture progression over time. Both can be premonitory signs of rockfalls. Therefore, rock face monitoring and surveying is essential for a better understanding of the instability mechanisms.

1.3. Purpose and contents

After those events, a Risk mitigation plan was started in order to implement a sustainable risk management strategy. A 3-year phase is currently underway (2014-2016). The installation of an early warning system (EWS) is not feasible at the present state of experience in this site. Thus, several monitoring techniques have been tested in the Montserrat area.

The final goal of the present Plan is to understand the rock mass behaviour and the failure triggering factors, and to study the progressive development of instability. The suitability and precision of each technique for different purposes will be obtained as well. Finally, the monitoring systems in use will aid in setting priorities for stabilization works.

For the current first phase, four monitoring techniques were selected. The objective of this paper is to explain the implementation of the techniques along with their results. The techniques and each test performed in Montserrat during 2014-15 are introduced in section 2: Total Station (2.1), rock joint instrumentation (2.2), Terrestrial Laser Scanner, TLS (2.3), and Ground-based Synthetic Aperture Radar, GbSAR (2.4). Then, in section 3 the results are analyzed and discussed. This section finishes with a comparison of the different techniques. Finally, some conclusions summarize the main points of the Montserrat monitoring so far.

2. Monitoring techniques

Landslides are commonly monitored and several early warning systems have been implemented successfully, because ground displacements often develop gradually before the failure [Zvelebil and Moser 2001], [Oppikofer 2009], [Intrieri *et al.* 2012] and [Crosta *et al.* 2014]. Recently, researchers have reported using remote sensing tools such as ground based LiDAR to detect pre-failure rockfall deformations [Abellán *et al.* 2009], [Royán *et al.* 2015] and [Kromer *et al.* 2015]. However, at Montserrat, it is particularly difficult to implement such an approach, because the rock mass is very stiff and apparently brittle: detachment is expected to occur at low strain. For this reason, high

precision measurements are needed. The goal of the monitoring action during the current 3-year plan is to improve knowledge of rock mass behaviour and understand the progressive development of instability, as in [Arosio *et al.* 2009] and [Royán *et al.* 2014]. Thus, in 2014-15, different pilot tests were performed to check the applicability of several techniques depending on each case and site. After the analysis and comparison of the preliminary results [Janeras *et al.* 2015], new monitoring tests are under development until 2016. For the current first phase, four monitoring techniques were selected with different spatial resolution and temporal acquisition (continuous vs. discontinuous) as seen in table 2. On the one hand, Terrestrial Laser Scanner (TLS) or LiDAR and Total Station measurements have been applied until now as discontinuous monitoring over time following periodic surveys. In contrast, with Ground-based Synthetic Aperture Radar (GbSAR) a continuous campaign has been performed as a pilot test. Finally, a network of rock joint instrumentation is being developed as real time monitoring. These four techniques and each test performed in Montserrat during 2014-15 are introduced in subsections 2.1 to 2.4, and their results will be summarized in section 3.

Table 2. Overview of the four monitoring techniques used in the pilot tests.

		Temporal domain	
		Continuous	*Discontinuous*
Spatial domain	*Continuous*	Ground Based Synthetic Aperture Radar	Terrestrial Laser Scanner
	Discontinuous	Rock joint instrumentation	Total Station

2.1. Surveying Total Station

The monitoring with Total Station is the simplest technique presented here. It was envisaged as a low-cost approach to monitor a small number of points on a potentially unstable block. In principle, this approach is discontinuous in the time domain as the measurements are carried out during periodic campaigns.

The Cadireta rock needle or block (figure 5) was used as a demonstration to adapt the method and assess its performance. It is a block of about 8000 m^3 overhanging over the hillslope. It presents a potential risk to a number of trails and to climbers visiting the area, and the local road that surrounds the mountain along the north flank [Cabranes 2015]. Here, our main goal has been to test the monitoring method.

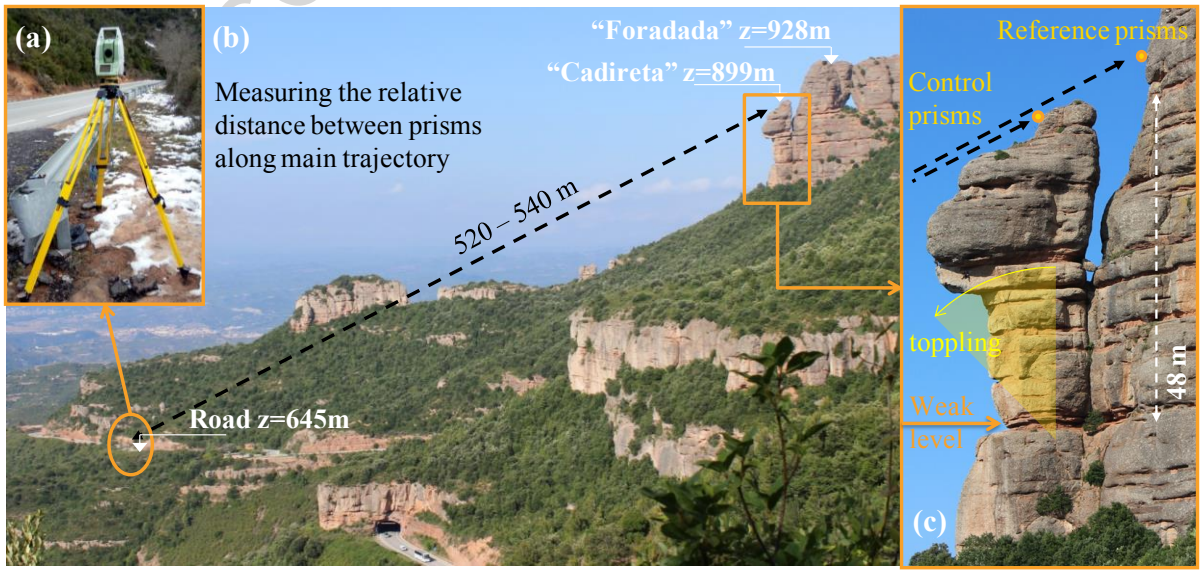

Figure 5. Leica TM30 Total Station used to survey the Cadireta rock needle (a). Lateral view of the slope from the base station to the Cadireta, where elevations are annotated in m.a.s.l. (b). In the zoom picture (c) the expected instability mechanism is shown. Measurement points on the block and the rear

wall are equipped by standard circular prism and mini-prism for monitoring the relative variation on the measured distances.

A convenient place for setting up the Total Station was the road below the block. From there, the measurements were made over a set of prisms distributed over the upper part of the block and others attached to the rear wall, used as references (figure 5). As expected, the large distance between the Total Station and the block (520-540 m) did not allow high precision measurements of the coordinates of the prisms. The angular precision (about 1 arc second, i.e. 0.3 mgon) produced a significant error in the coordinates (3 to 5 mm). In contrast, the measured distance is more robust (precision about 1 mm). The distance difference between points ($D_{ij} = D_i - D_j$) is used to monitor displacement. D_i is the distance to a control prism, whereas D_j is the distance to the closest reference prism. Several tests have been carried out at the Cadireta site to confirm the precision of the method. The results show that the Standard Deviation of ΔD_{ij} is close to 0.8 mm, whereas the Standard Deviation of the 3D coordinates is roughly 5 mm.

This Total Station procedure has two additional advantages: the first is related to the correction of the raw distances to take into account ambient factors. In such mountainous terrain it is very difficult to measure the air temperature and humidity due to its great variability depending on time and elevation (further discussed in section 2.4 as a critical factor for GBSAR). Through the difference of similar measurements, D_{ij} is quite insensitive to small inaccuracies in the measurement /estimation of the mean temperature and humidity along the laser beam. Secondly, our procedure is also robust in front of small "changes" in the base point; these spurious "movements" might be produced by an eccentricity in the setup of the Total Station or by a real settlement of the ground in the vicinity of the base benchmark.

When editing this article, we have just acquired the first 6 seasonal campaigns after completing only one year of monitoring at the Cadireta site; seasonal monitoring is planned to cover several years in order to characterize the natural behaviour of this block.

2.2. Monitoring of rock joints

Another applied monitoring technique consists of the installation of sensors on the rock mass surface that directly measure the relative movement of discrete points across a joint of discrete blocks; when combined with an automatic data acquisition system, the method can provide high precision data and high temporal resolution, also in real time.

In Montserrat, an experiment with this monitoring technique was started in September 2010 to monitor the movement of a huge rock mass (A3-6 block) above the rack railway. To that end, 3 extensometers were installed together with an air temperature sensor to measure the movement of this mass relative to the massif. These sensors were wire-connected to a CR800 Campbell Scientific (CS) datalogger provided with a photovoltaic power system and a third generation of wireless mobile communications system (3G) for remote access. Data are acquired at one sample per minute and stored locally every 30 minutes. This system provides continuous data with ±0.01 mm of resolution and ±0.02 mm of precision.

Unfortunately, after the first year, the project was discontinued for the next 3 years and it was not properly maintained, leading to some gaps in the time series data. With the current plan, this test site has been reincorporated into the newly created network. Despite the gaps, we have currently reached a five-year monitoring period enabling analysis. Some results will be given in section 3.2. Data show elastic displacements, with a full range of about 2.5 mm, clearly related to temperature fluctuations. With newly appropriate maintenance, the system keeps providing continuous data, demonstrating its feasibility for long-term operation. However, a major disadvantage of such monitoring technique is the effort and the cost of cabling the sensors up to the datalogger, especially at the Montserrat massif where this task must be carried out by qualified rope access staff.

A project to extend monitoring in Montserrat massif to other potentially unstable blocks began in 2014, following the priorities suggested in [Janeras *et al.* 2011] and [Gallach 2012]. Taking advantage of the previous experience with the A3-6 block, new sensors were installed during the year to monitor the movement of a cluster of blocks called Diable, where a rockfall crushed a monastery dependency in the 16th century, killing four monks, as has been recovered from historical documents (figure 6). From this event remains the overhanging morphology of the Diable block.

Three different types of displacement sensors have been installed: 13 crackmeters to measure distances between close anchor points, 5 wire crackmeters to measure distances between distant anchor points, and 4 tiltmeters which use MEMS accelerometers mounted on aluminium beams to measure vertical displacement between the anchor points of the beam (figure 6). During the first operational year, the wire extensometer malfunctioned, but it was later corrected by the manufacturer. We also learnt that the bar-tiltmeter is very sensitive to environmental conditions derived from the works on the cliff. For these reasons, both types of sensors are still under testing and revision. Only the crackmeters currently provide reliable data.

To reduce the cost and effort of cabling sensors to one or several CS dataloggers, and also its visual impact, a new concept of distributed wireless data acquisition network has been implemented, based on ZigBee loggers (ZBLoggers) following other recent developments in wireless sensor networks (WSN) for rock mechanics under different environmental conditions ([Alippi *et al.* 2008], [Hasler *et al.* 2008], [Beutel *et al.* 2011] and [Kawamura *et al.* 2014]). A ZBLogger is a low-power, low-cost system of ICGC's own design with 3 single-ended (or 1 differential plus 1 single-ended) input channels and a wireless connection, based on ZigBee protocols (IEEE 802.15.4 standard), which can communicate with other ZBLoggers as well as with the CS datalogger. Eight LR6 1.5V rechargeable batteries and a solar cell of 0.96 W provide the system with enough energy for long-term operation (5-10 years, depending on battery life in terms of charging cycles).

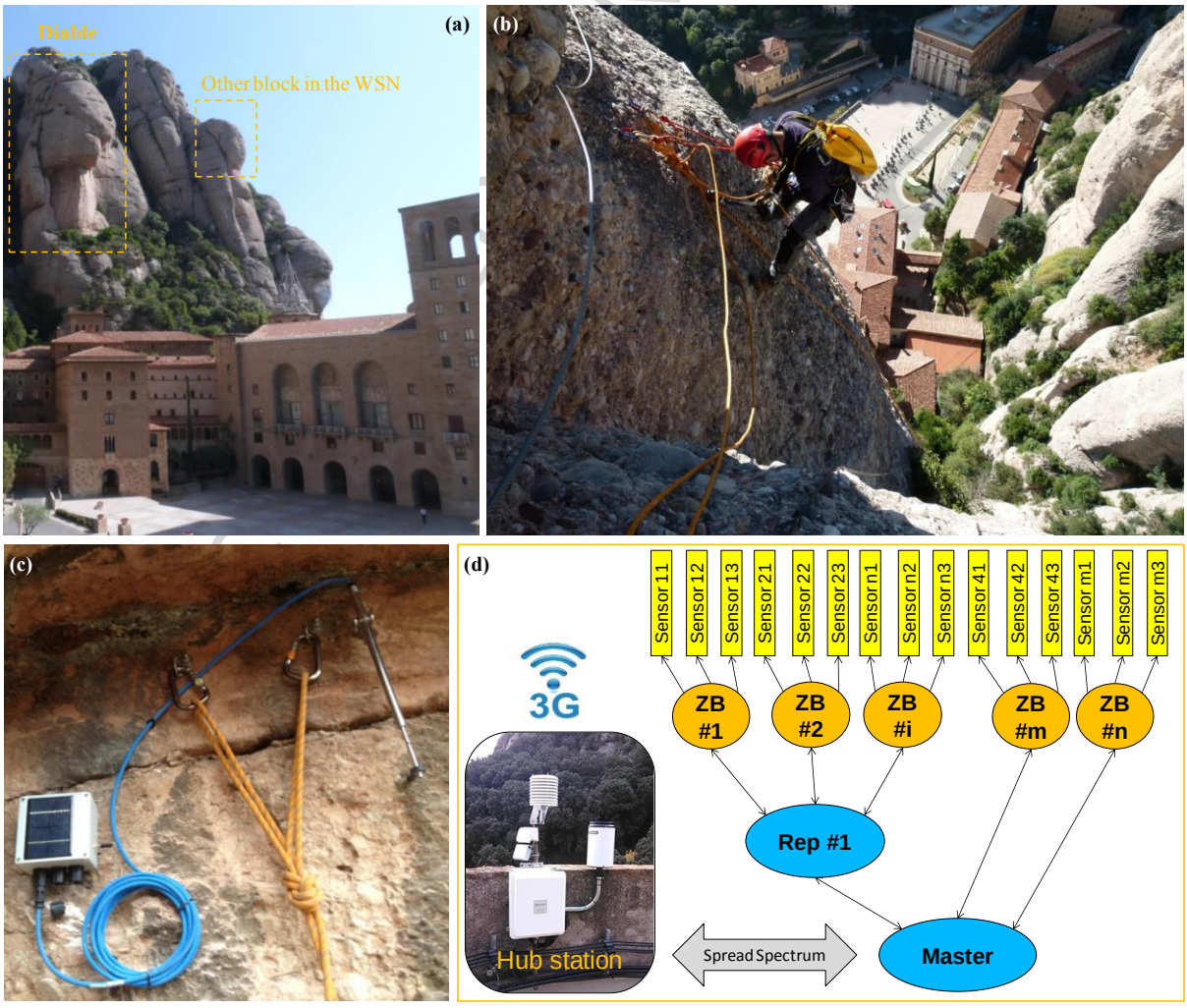

Figure 6. Location of the Diable blocks above the monastery (a). Monitoring of the block's joints with crackmeters, bar-tiltmeters and wire-extensometers installed using rope access works (b). Configured network based on ZBLoggers connected to sensors (c) and wireless communication through repeaters and a master to the hub station connected to Internet by a 3G mobile communications system (d).

ZBLoggers digitize the signal of input channels, taking 1 sample each 10 minutes, with a 16-bit sigma-delta A/D converter. Data from a ZBLogger can be sent directly to a datalogger across the wireless network (800 m maximum range in case of direct line of sight), or via other ZBLoggers acting as repeaters (figure 6). The average of 3 consecutive samples is recorded every 30 minutes. Once data are stored inside the datalogger, they are sent to the Data Centre via Internet, and archived into a database. Finally, "NetMon", a proprietary web-based tool developed by ICGC, allows available data to be harnessed effectively. After the first months of tests in Diable, a second version of improved ZBLogger was applied during 2015/16 in other blocks, and the system remains operational and ready to be extended to further blocks, although some refinements are still desirable in order to reach a more stable system.

2.3. Terrestrial Laser Scanner

The monitoring of several rock cliffs of Montserrat Mountain was carried out with an ILRIS-3D (Optech) Terrestrial Laser Scanner (TLS) (figure 7). The laser beam is reflected by the rock slope surface, which means that no artificial reflectors are necessary. The instrument calculates the distance to an object, also called range, using the time-of-flight of the laser pulse [Petrie & Toth 2008] and [Lato *et al.* 2012]. According to specifications, ILRIS-3D can reach a maximum range of 700 m for natural slopes and decreases as a function of the material reflectivity and incidence angle to the object. The datasets acquired by this device can provide an accuracy of 7 mm at a distance of 100 m, according to the manufacturer's specifications. The device can acquire a great number of points, also called point clouds, in a very short time (2,500 points/s), which provides a high density of information (around a few thousand points per square metre).

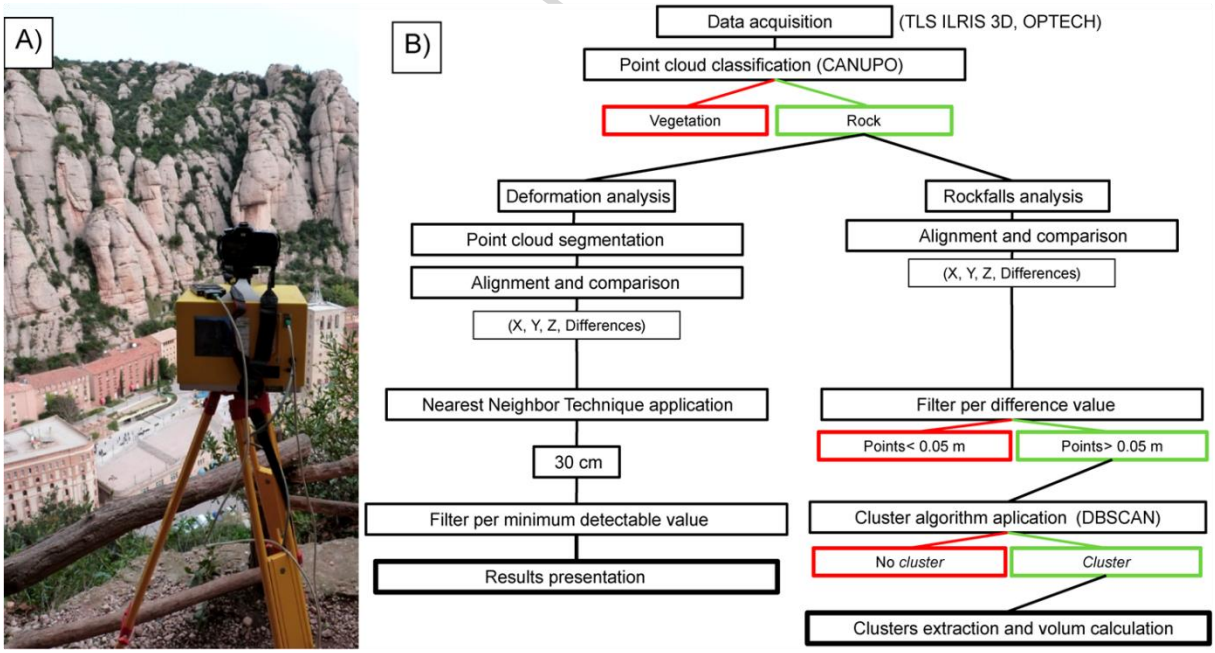

Figure 7. Data acquisition with the TLS equipment in the panoramic point of view to the Monastery cliff (a). Workflow of the processes applied to detect deformation and rockfalls (b) (adapted from Abellán *et al.*, 2009, Tonini & Abellán, 2014 and Royán, 2015).

The time series of the TLS data sets in Montserrat Mountain are the longest of all the techniques presented in this article, so it is of special interest in detecting both rockfalls and deformation from years ago. In Degotalls area the first survey was performed in May 2007 and 14 different fieldwork campaigns were conducted until December 2015 (figure 8), making it a monitoring period of 3136 days. Two scanning stations are used to cover the two different rock cliffs that make up the Degotalls study area: Degotalls N (north-facing wall) and Degotalls E (east-facing wall). The mean range between the scanning stations and the rock faces is 250 m. Another study area corresponds to the Monastery cliff, the rock face behind the sanctuary and monastery buildings, where the first survey

from a panoramic point of view (Fra Garí) was performed in February 2011 and 12 surveys were carried out until December 2015 (figure 8), reaching a monitoring period of 1760 days. From this lookout point, the mean distance is also around 250 m. Moreover, in July 2015 a new series of TLS data was started in the Montserrat Monastery area from a closer view. Two new scanning stations were set up on the rooftop of a central building and in the upper part of a tower in order to reduce the scanning range down to 143 m in two specific sectors of this rock face over the Monastery area, one of which, the Diable block, was presented in the previous section. A second survey from these new stations was carried out in December 2015, totaling 156 days of monitoring.

TLS data pre-treatment consisted of: a) classification of each point cloud using CANUPO application [Brodu & Lague 2012] in order to filter vegetation areas; b) alignment with the previous dataset to detect rockfalls between periods, or with the first dataset to detect accumulated displacements. This procedure was carried out through a preliminary identification of homologous points and a subsequent minimization of the distance between point clouds using the Iterative Closest Points (ICP) algorithm [Chen & Medioni 1992]. Step c) corresponds to the comparison of the different TLS datasets based on the quantification of the distances between each pair of datasets which was performed using a conventional "point-to-surface distance" methodology implemented in IMInspect software, InnovMetrics PolyWorks v.10.0.

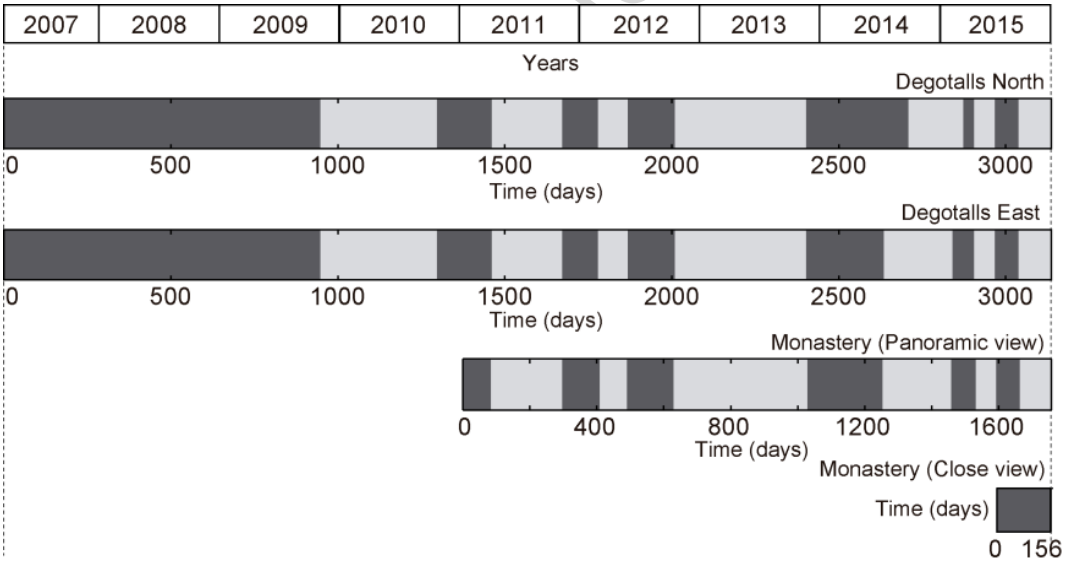

Figure 8. Time series relating to the TLS campaigns obtained from Degotalls and Monastery study areas.

In order to detect changes in the rock face including both rockfalls and surface displacements, two different processes were applied (figure 7). On the one hand, to detect centimetre-scale displacements, a filtering technique based on the large number of points of the TLS point clouds was applied. This procedure is based on the proposal by [Abellán *et al.* 2009] and other similar works (Kromer *et al.* 2015), and in brief consists of searching the nearest neighbour points around each point of the point clouds in a maximum radius (30 cm in this study) and the median calculation of the differences between datasets. As a result of this process, called Nearest Neighbour 3D (NN-3D), the minimum detectable deformation value was reduced down to 1 cm.

On the other hand, in order to detect rockfalls, an algorithm to find clusters based on the methodology proposed by [Tonini & Abellán 2010] was applied. This process mainly consists of three steps: a) filtering the differences not corresponding to rockfalls; b) application of DBSCAN algorithm (Density-Based Spatial Clustering of Applications with Noise [Ester et al. 1996]) to remove noise and find different clusters; c) quantification and volume computation of the single clusters detected corresponding to single rockfalls. Given that the minimum value of differences used was 5 cm, the minimum number of required points for a cluster was defined as 10; the average point spacing of the scans was between 7 cm and 9 cm; and the minimum detectable rockfall volume was defined as 0.001 m^3 (equivalent to 2.5 kg of conglomerate). This level of detection is considered in the Degotalls

and Monastery panoramic view study areas, but in the case of the close view of the Montserrat Monastery study area this level is lower because of the range reduction. Thus, the minimum value of differences was reduced down to 3 cm, allowing the detection of rockfalls of one order of magnitude smaller.

2.4. Differential SAR interferometry

In 2014-2015, a first extensive measurement campaign using a Ground Based Synthetic Aperture Radar (GBSAR) was performed in Montserrat. Data collected by this kind of SAR sensors produces terrain reflectivity images, which can be processed by means of differential SAR interferometry (DInSAR) algorithms for the monitoring of deformation episodes, with millimetric accuracy [Gabriel et al. 1989] and [Massonnet & Feigl 1998]. DInSAR techniques are based on the use of the phase-differences between multitemporal pairs of complex SAR images of the same area of study so as to obtain the terrain displacement projected onto the line-of-sight (LOS) direction.

The aim of the experiment was to take advantage of the wide area coverage (2 km long and 1 km wide) and its high sensitivity to displacement detection (on the order of a millimetre). GBSAR sensors are used for the precise monitoring of small-scale phenomena. This kind of instruments have been used for several applications such as landslide monitoring, subsidence hazards in urban areas, volcano monitoring, etc. [Corominas *et al.* 2015] and [Iglesias *et al.* 2015], when a classical Orbital DInSAR system cannot be used due to the bad geometric orientation of the scenario or because the revisit time of the Spaceborne sensor is not short enough to monitor the deformation. The main characteristics of the UPC RiskSAR equipment (GBSAR) in two configurations are summarized in table 3.

Table 3. Main characteristics of the two types of RiskSAR equipment (GBSAR systems of RSLab of UPC).

Parameters	**X-band**	**Ku-band**
Carrier Frequency	9.65 GHz	17.5GHz
Modulation	triangular CW-FM	triangular CW-FM
Signal bandwidth	100MHz	200MHz
Polarization	Full polarimetric combinations	VV single polarization
Range resolution	1.5 m	0.75 m
Azimuth resolution	~10 mRad	~5mRad
Pixel size at 200m	3 m^2	0.75 m^2
Range coverage	3Km	1.5Km
Azimuth coverage	±30º	±30º

The instrument RiskSAR at X-band was placed in the Guilleumes test site a few metres upslope from the rack railway, at an altitude of 380m (figure 9). It was pointed south and inclined 25º upslope, pointing to two different main rock cliffs, 400 and 800 metres from the radar. The system operated autonomously but it could be remotely controlled via wireless link. A sequence of one measurement per hour was programmed during the 5-month experiment (October 2014 - February 2015).

Figure 9 shows the reflectivity image covered by the sensor projected on topography. The strong reflectivity response corresponding to the main rock cliffs can be observed in the image. Different radar calibrators were deployed along the slope to facilitate the image geocoding process. A test with a Polarimetric Active Radar Calibrator (PARC) over a millimetric positioner was performed to validate system capability in order to detect small displacements at 600 m of distance (figure 10). Negligible differences can be seen between the real position of this active target when a displacement is imposed and the position retrieved by measurements, which are due to the thermal stabilization of the internal electronics of the PARC.

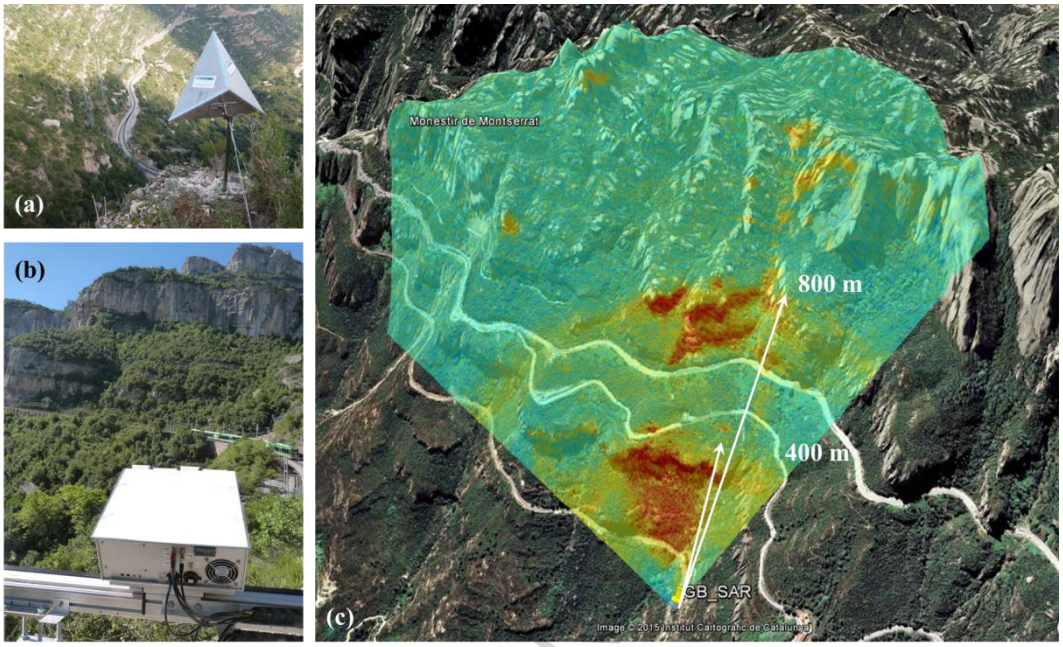

Figure 9. Radar setup from the Guilleumes site on the north flank of Montserrat (b). Radar reflectivity image on Google Earth map (c). Reflector corner placed on the top of the first cliff at 534 m.a.s.l. (a).

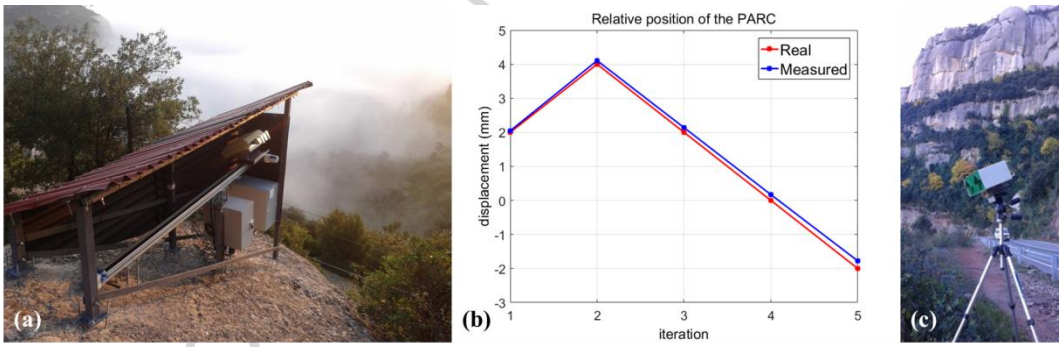

Figure 10. RiskSAR system placed at the Guilleumes site with weatherproof cover for use in short campaigns (a). Peformance test with Polarimetric Active Radar Calibrator (PARC) placed next to the upper road at 642 m.a.s.l. (c) and displacement position retrieved after DInSAR processing when a displacement is applied to the PARC with the millimetric positioner on its base (b).

For this type of sensors, the atmospheric phase screen (APS) is the most relevant artefact of distortion on the interferometric phase. Hence, in order to apply any DInSAR technique to obtain reliable deformation maps, these atmospheric artefacts must be correctly estimated and consistently compensated as in [Pipia *et al.* 2008] and [Iglesias *et al.* 2014]. Unfortunately, this implies that an important set of measurements have to be discarded because of the accentuated atmospheric anomalies. Between each pair of images, a lineal drift of the differential phase along the radar range can be expected and easily compensated with SAR post-processing (figure 11.a). But at this site the measurement comparison frequently shows unwrapped differential phase distributions with any linear performance, which are difficult to compensate (figure 11.c and 11.d). These difficulties can often be encountered in mountainous areas due to fog, rain, stratification and temperature inversion, as in this case, worsened by the radar measurement direction uphill and tangent to the forest. The configuration of the Llobregat river basin leads to frequent atmosphere stratification on the north flank of Montserrat Mountain with the fog roof altitude varying from 450 to 650 m (figure 11.b).

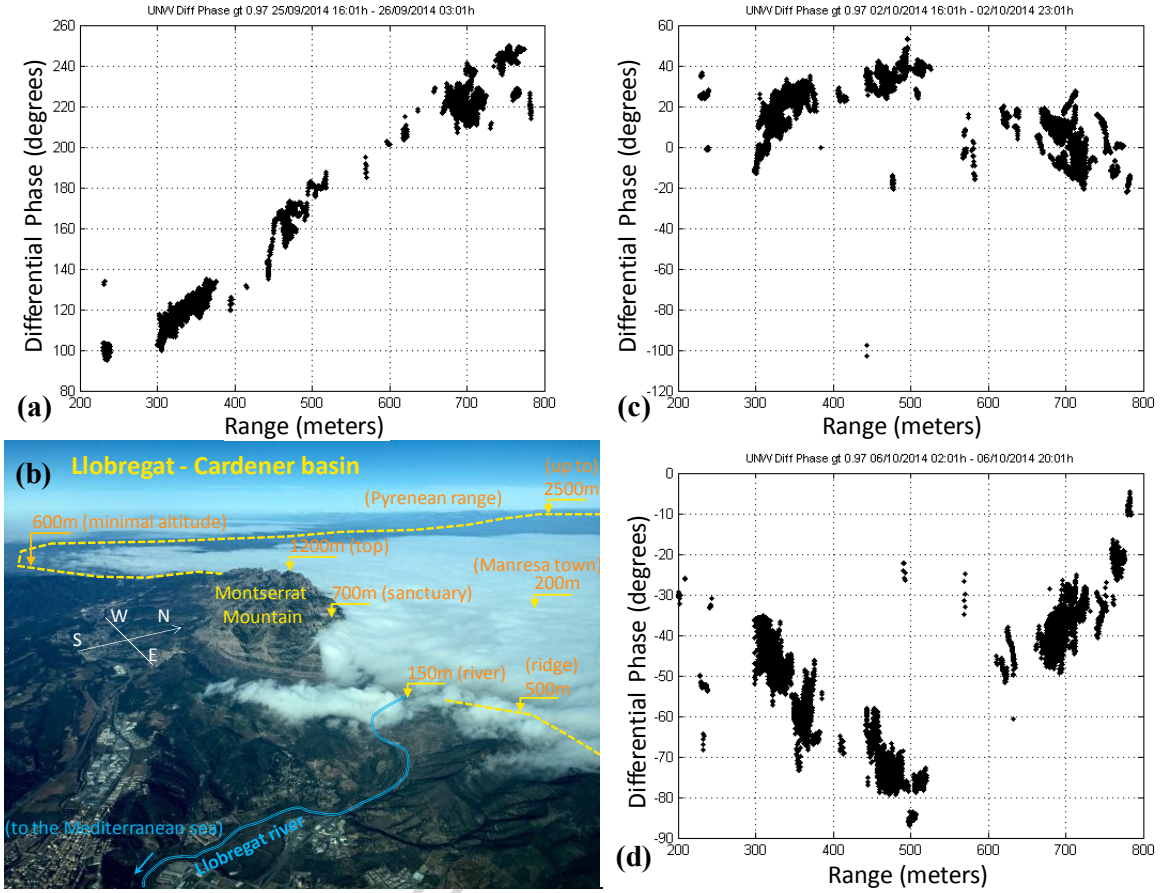

Figure 11. Three different unwrapped differential phase distributions between a pair of images as a function of radar range: a) the differential follows an expected linear performance of the differential phase with regard to the radar range, which can be easily compensated with SAR post-processing; c) and d) two other situations where graphs show different nonlinear performances, which are difficult to compensate. The aerial image (b) shows a typical atmospheric situation at this section of the Llobregat river leading to the nonlinearity of the previous graphs, which configures a great difficulty in applying GBSAR monitoring to the north flank of Montserrat Mountain.

The first experiment at the Guilleumes site has retrieved limited results (as explained comparing the results in the next section) due to these multiple difficulties related to the atmospheric disturbance. Consequently, a second test was performed at the end of 2015 to analyze the suitability of two other radar station locations in the Monastery area and the Degotalls wall, both at an altitude higher than 650 m.a.s.l. and closer to the slope, enabling the application of the Ku-band system (table 3). The first impression of the resolution comparing X-band and Ku-band systems is shown in figures 12a and 12b. At the Degotalls site there is clear improvement of pixel size in the reflectivity map from X-band to Ku-band, together with a better delimitation of the scenery in coherence and the interferometric phase map. Taking into consideration the antecedent rockfalls detached from this rock wall (figure 4) and the results of the TLS presented below, X-band could have enough resolution to detect displacements in large blocks (more than 10 m^2 of visible face). At the Monastery site, the improvements provided by the Ku-band regarding X-band are better appreciated in all 3 types of maps. Because the relief is more complex and a better localization of an eventual movement is required, the Ku-band device will be considered for further tests.

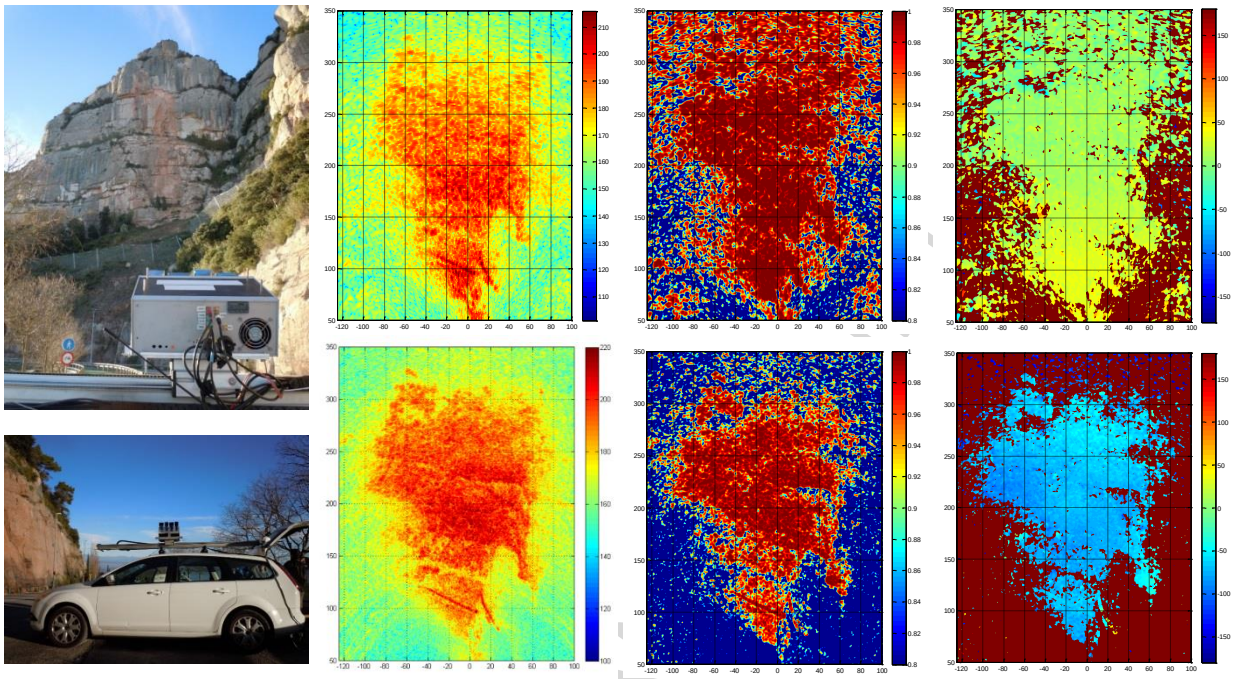

Test site | SLC (reflectivity map) | Coherence map | Interferometric phase map

Figure 12a. Radar performances obtained by the test for Degotalls N wall, comparing X-band (upper row) and Ku-band (lower row) in terms of reflectivity, coherence and interferometric phase maps.

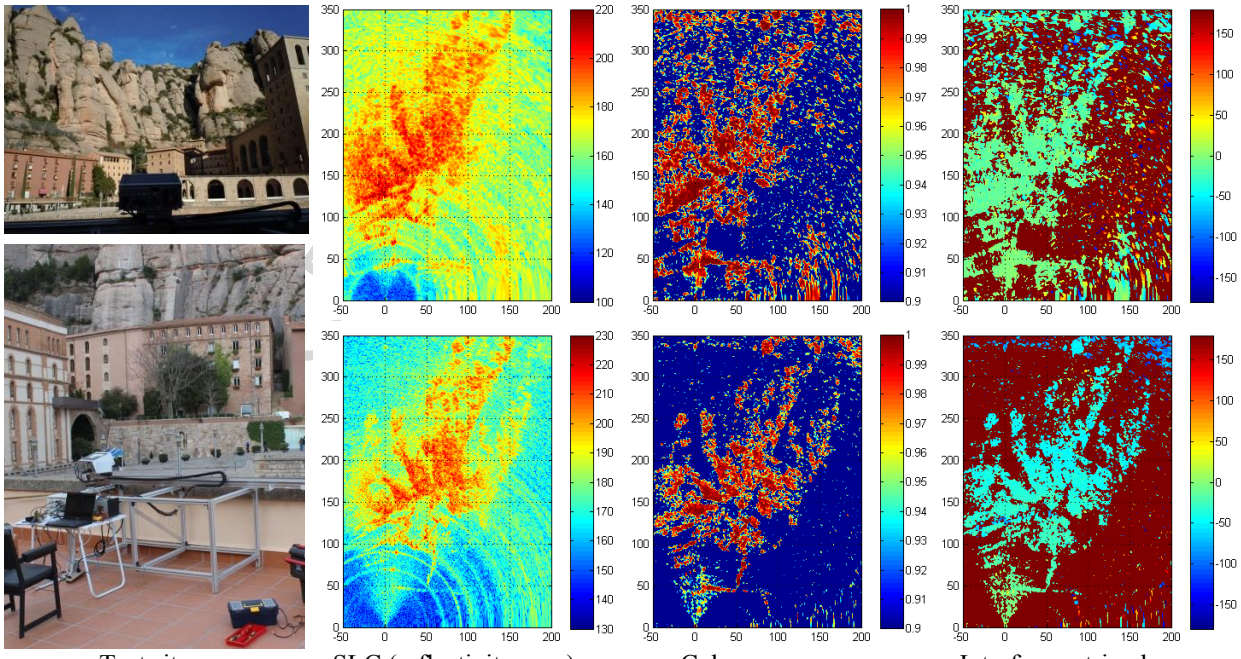

Test site | SLC (reflectivity map) | Coherence map | Interferometric phase map

Figure 12b. Radar performances obtained by the test for the central part of the Monastery cliff, comparing X-band (upper row) and Ku-band (lower row) in terms of reflectivity, coherence and interferometric phase maps.

3. Analysis of the monitoring results

Although the four monitoring techniques presented in the previous section are in the test phase, some interesting results have been gathered so far, which permit gaining certainty of the suitability of the techniques for rockfall monitoring in Montserrat. With the available data, mainly the TLS, the assessment of rockfall activity is carried out in subsection 3.1. Looking at the complete set of results,

some recoverable or 'elastic' deformation can be identified (subsection 3.2), which is related to the cyclic response of the massif to daily or yearly thermal effects. On the other hand, some cumulative or irrecoverable deformation is also evident in some results. This kind of permanent displacement that might precede a major failure is analyzed in subsection 3.3. In the three quoted subsections, some advantages and drawbacks of the four techniques will be highlighted, whereas the main features will be summarized in the comparison section, 3.4.

3.1. Rockfall activity assessment

TLS multi-temporal comparison makes it possible to detect rockfalls that were not recorded by conventional observation, and also to calculate their volume. In contrast, GBSAR is not able to clearly detect these rapid changes of landscape, because the comparison is made in terms of the phase of the signal. The summary of rockfall activity detected in the different study areas is presented in table 4. Among all detected rockfalls, only two events located at Degotalls N were characterized by volumes greater than 1 m^3 (8 and 883 m^3). The other unnoticed events were characterized by a small magnitude, with volumes ranging between $1 \cdot 10^{-3}$ and 0.732 m^3, and associated with the disaggregation of pebbles and failure of small slabs.

The most remarkable information in table 4 is the large number of rockfalls detected in the Degotalls N wall (n = 218). This high number of events is derived from the impacts at the lower part of the wall caused by the rockfall that occurred in December 2008 with a total volume of 883 m^3. It is also remarkable that, due to the reduction in the level of detection in the Montserrat Monastery close view study area (> $1 \cdot 10^{-4}$ m^3), the annual unitary rate of the rockfall is significantly higher in this area than in the other three.

As an example of the spatial distribution of rockfalls, the location of the events detected in the Montserrat Monastery rock face (panoramic view) and in the Degotalls E cliff is shown in figure 13a and b. Moreover, the rockfall unitary rate over time for both rock faces can be observed in figure 13c. Both the number of events per square metre and the annual unitary rate of the rockfall are greater in the Degotalls E wall, showing the higher rockfall activity of this rock face.

Table 4. Rockfall activity characterized with Terrestrial TLS expressed in the number of rockfalls detected per period of analysis in each study area.

	Degotalls N	Degotalls E	Monastery (panoramic view)	Monastery (close view)
Days of monitoring	3136	3136	1760	156
Area of analysis (ha)	1.44	1.60	3.26	1.47
Mean scan range (m)	256	220	250	143
Level of detection (m^3)	$1 \cdot 10^{-3}$	$1 \cdot 10^{-3}$	$1 \cdot 10^{-3}$	$1 \cdot 10^{-4}$
Number of rockfalls	218	121	112	24
Rockfall annual unitary rate (number / (year·ha))	17.62	8.80	7.12	38.20

The rate of activity seems to be quite uniform over time, but from 2015 the sampling frequency was increased in order to monitor seasonal variability. After the first year of this configuration, an increase in activity was detected in both study areas during the last quarter, probably corresponding to the intense rainfall on 2/11/2015 that detached a shallow landslide of the colluvial soil on a nearby slope. But further data under different conditions are necessary to extract conclusions. This inventory information (volume and event date) gathered in the TLS monitored areas is of paramount importance in order to adjust the magnitude – cumulative frequency relationships, as shown in figure 13d for both areas. Similar behaviour is seen with a slight difference in the slope, which is consistent with the fact that the nature of the rock mass is the same. This work is currently under development (Royán *et al.*, 2016).

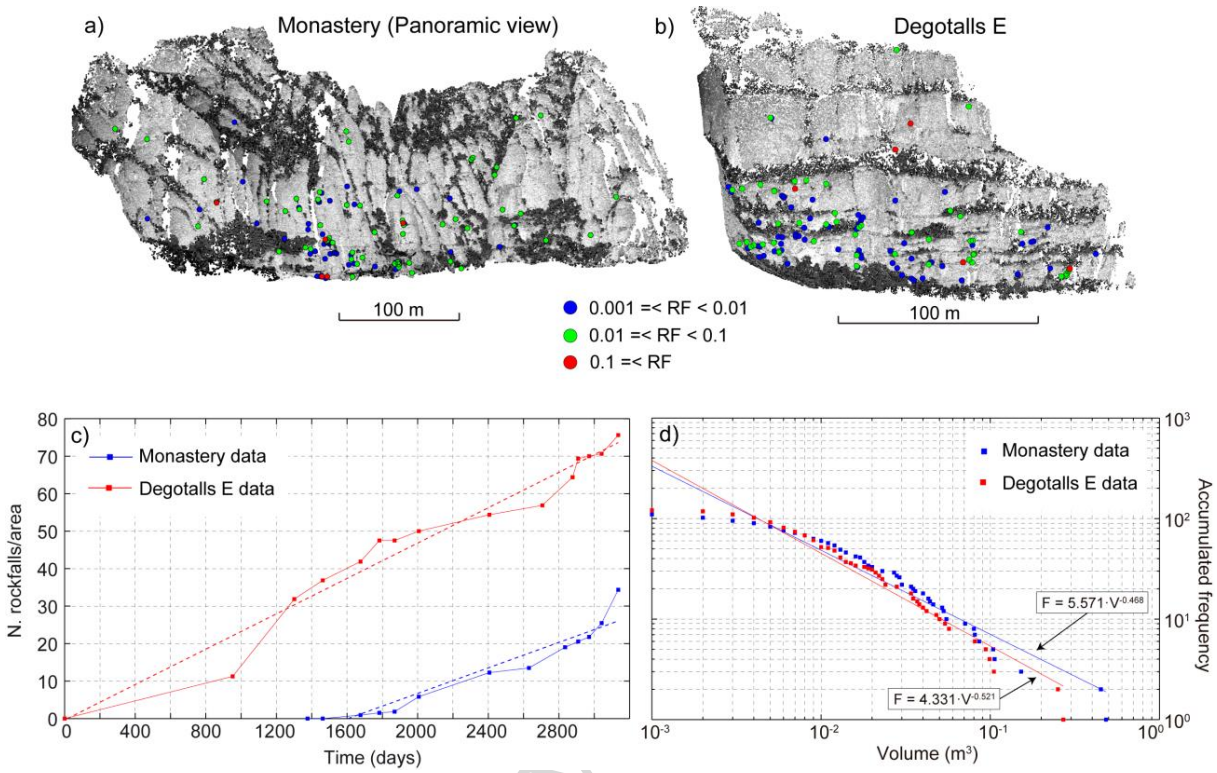

Figure 13. Rockfall detection with TLS monitoring in the Monastery (a) from the panoramic viewpoint and Degotalls E (b) study areas, where RF is the rockfall volume in m3. c) Accumulated number of rockfalls per hectare of outcrop surface for both areas from the first campaign for each area until December 2015. d) The statistical distribution of rockfall volume constitutes the magnitude – cumulated frequency relationship for both areas.

3.2. Rock mass cyclic deformation

The longest register of joint monitoring is obtained for block A3-6 situated at the top part of the cliff over the rack railway (Figure 14). The instrumentation was installed in 2010, but the incidents explained in section 2.2 led to some gaps in the time series data. However, in 2015, this monitoring station and its register were restored with sufficient data. to assess the displacement trends over 5 years.

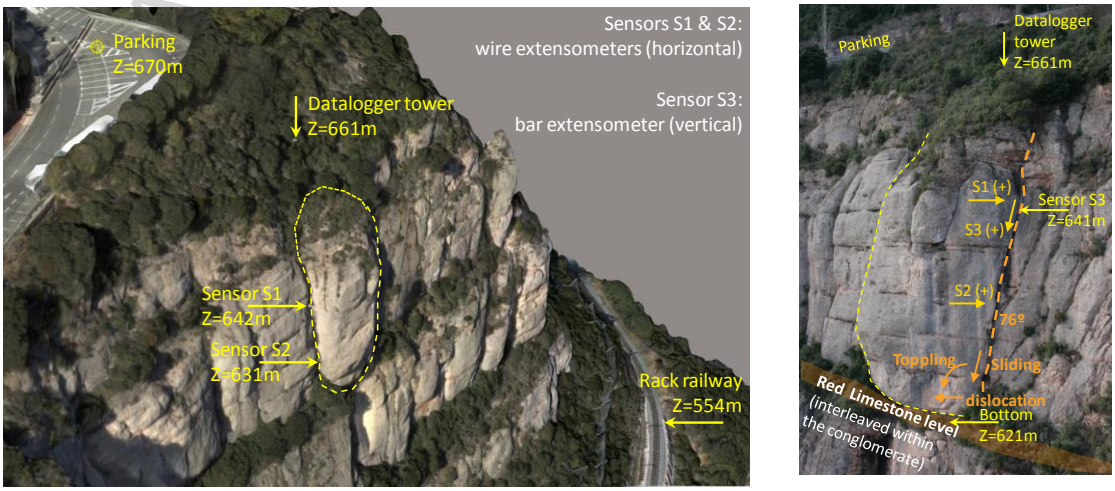

Figure 14. The rock block A3-6 in the upper part of the cliff between the road and the railway seen on a photogrammetric 3D model obtained by ICGC (left) with the position of the joint sensors. The structural disposal, the instability mechanism and the reading sense of the sensors are shown on the lateral view (right) similar to a section orthogonal to the rear joint.

These data clearly show the annual cycle as well as daily oscillation (figure 15), as can be clearly identified with a FFT analysis. This behaviour can be linked with the thermal deformation of the superficial part of the rock mass, including the analysed block, but the thermal effect on the sensors must also be considered. The mean amplitude of annual oscillation is 2.0, 1.0 and 1.3 mm for sensors S1, S2 and S3 respectively, and 36.7ºC oscillation for the temperature (figure 15). Sensor S3 (a bar-extensometer in the sliding direction of the rear joint) shows completely elastic behaviour, recovering its original value after the annual cycle. In contrast, sensors S1 and S2 (wire extensometers measuring the aperture of the rear joint at the upper and medium part) have a slight tendency to accumulate displacement at a rate of 0.169 and 0.065 mm/year for S1 and S2 respectively. According to the sensors' positions shown in figure 15, these strain rates correspond to a toppling movement of 5.1E-5 rad/year with a joint closure of 0.15 mm/year at the base and without any significant sliding, so equivalent to a rotation around a horizontal axis placed in the joint plane at 624 m of altitude. Due to the small scale of the strain, there could be a creeping process of weakening of the limestone level in the base, and an infill in the rear joint that prevents its fully elastic recuperation. To determine if this mechanism is leading to a long-term toppling failure, it must be monitored further to allow a second order analysis of a longer time-series by means of acceleration.

Similarly, in the Cadireta site, as a preliminary result of Total Station monitoring, we have measured 8 mm cyclic deformation of the top of the rock needle within one year. The seasonal behaviour of the Cadireta seems to be similar to that described for the A3-6 block, but further annual cycles with seasonal measurements are needed prior to drawing any conclusions. The magnitude of movement of each rock block or needle will probably be related to its structural disposal and degree of free movement according to the constraints on the discontinuities delimiting the block geometry.

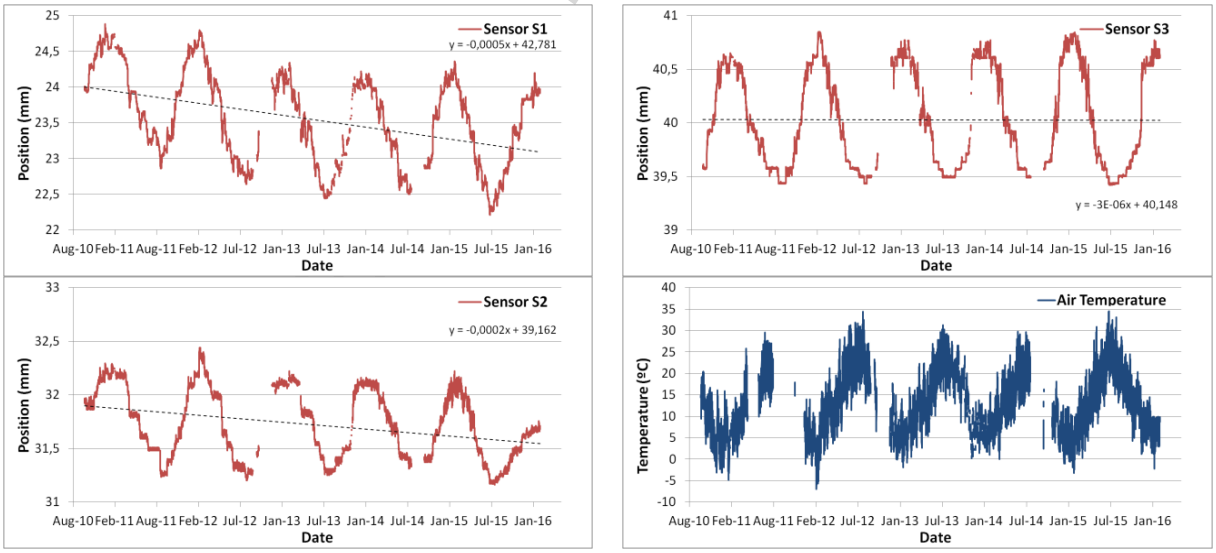

Figure 15. 5-year register of monitoring of rock joints in block A3-6, where sensors S1 and S2 are wire extensometers orthogonal to joint, and sensor S3 is a bar extensometer parallel to joint.

The thermal effect on sensors is expected to be mainly related to air temperature with rapid oscillation, whereas the rock mass response should be related to the temperature of the ground in depth, according to its different heat transfer rates. To improve knowledge of this issue, in the new instrumented block (Diable) thermistors have been installed inside the rock (at depths of 17 and 39 cm), as well as a pyranometer to measure solar irradiance (300 to 2800 nm) over the rock surface. The heat flux inside the rock mass over the first month of monitoring is shown in figure 16, but analysis of the data is only just starting. Further tests are under preparation to explore the exfoliation effect as done by [Collins & Stock 2016].

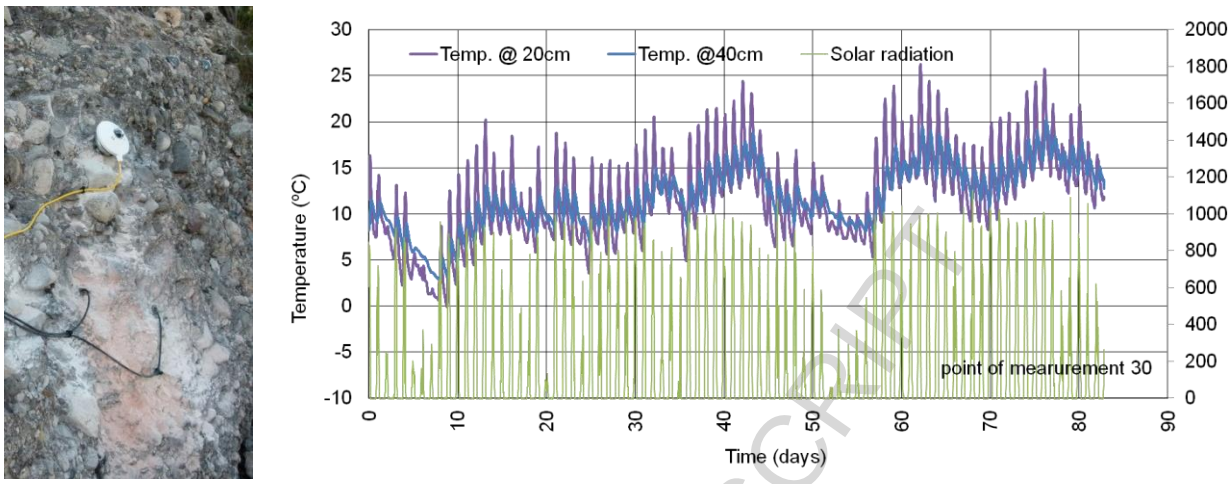

Figure 16. Register for the first 3 months in Diable block: temperature inside the rock mass at 17 and 39 cm, and solar net radiation in W/m^2, which sensors are shown on the left picture attached on the conglomerate wall.

The other remote sensing techniques (TLS and GBSAR) are currently not providing enough precision to resolve the level of millimetre scale deformation occurring in the rock mass. With the equipment in use and under present working conditions, we are reaching precisions of approximately 10 mm for TLS, and 3 to 5 mm for GBSAR with X-band at medium distances.. To improve the precision of both scanning techniques, on the one hand, a new test with GBSAR at closer distances and higher frequency (Ku-band) is planned in the Monastery or Degotalls cliffs, where the overlapping of different monitoring techniques appears more feasible. A first pilot test was performed as explained in section 2.4.

On the other hand, the close view of the central part of the Monastery cliff corresponds to 2 points added during 2015 for positioning TLS focused on 2 main sectors of interest. In this line of work, and specifically for the Diable block, no relevant displacement was observed (figure 17 a and b) when comparing both TLS scans lagged 156 days between 1/07/2015 and 4/12/2015. There are different artefacts produced by an increasing incidence angle, but they cannot be interpreted as movements in this study area. The minimum detectable value of displacement (two times the standard deviation, 2σ) was reduced from the 15 mm obtained in the panoramic view, to 6 mm obtained in one of the new close views (figure 17c). Reviewing the rock joint monitoring installed in this site, for the same period the 13 crackmeters have recorded displacements of up to 0.59 mm, with a mean value of 0.16 mm. It seems clear that this range of movement cannot be detected with remote sensing like TLS.

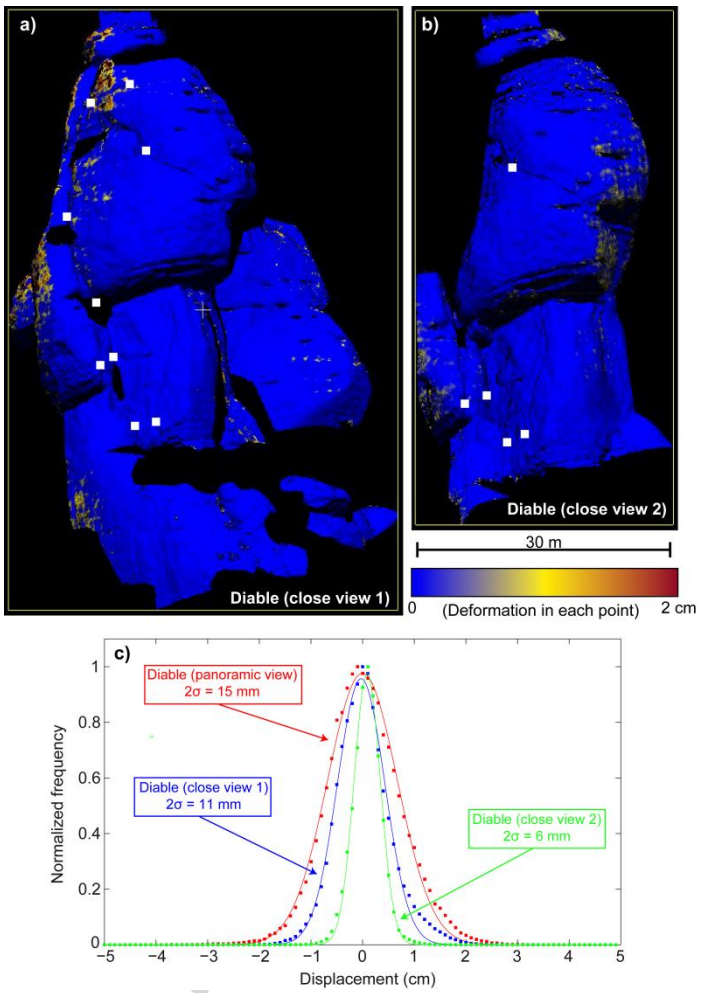

Figure 17. Result of TLS monitoring of Diable blocks from the close point of view 1 on a rooftop (a) and close point 2 at the top of a tower (b) comparing the campaigns of 1/07/2015 and 4/12/2015. Slight differences only appear where the line of sight is highly oblique to the rock surface. The white dots indicate the position of the contact sensors (crackmeters). At each scan station, both scans were acquired at the same hour of the day. In (c) the statistics of the range differences (apparent displacements) show the improvement in the detection threshold in relation with the panoramic station point.

3.3. Rock mass permanent deformation

TLS monitoring was able to detect precursory movement in two different blocks located in Degotalls N wall (figure 18). Block A instability was detected in the period from May 2007 to December 2009, after the big event in December 2008 and close to the large fallen mass. This movement was characterized by an initial displacement of more than 2 cm and a subsequent halt in the following periods (figure 19). This behaviour suggests that the movements have some kind of link to the great rockfalls of January 2007 and December 2008. Block A is a part of a rock remaining after the blasting works carried out in February 2007, but probably with a damaged equilibrium due to a worse reduction in rock strength than the mass removal pursued by these works. During a rainfall period related to several rockfalls, on 01/11/2008 a lateral wedge of the block became detached. From February to April 2009, a stabilization work with steel rope meshes and anchors was carried out. After this date, TLS measurements show oscillating behaviour fully compliant with a flexible-type retaining structure. This block is planned to be instrumented in late 2016 to confirm the appropriate function of the mesh.

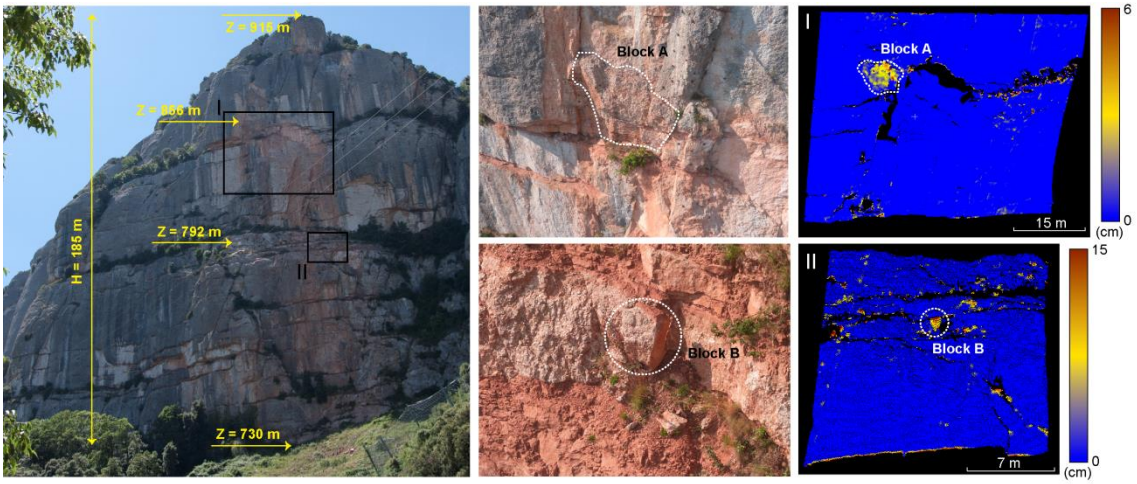

Figure 18. Location of the two blocks in the Degotalls North wall where displacement has been detected and their total amount measured with TLS.

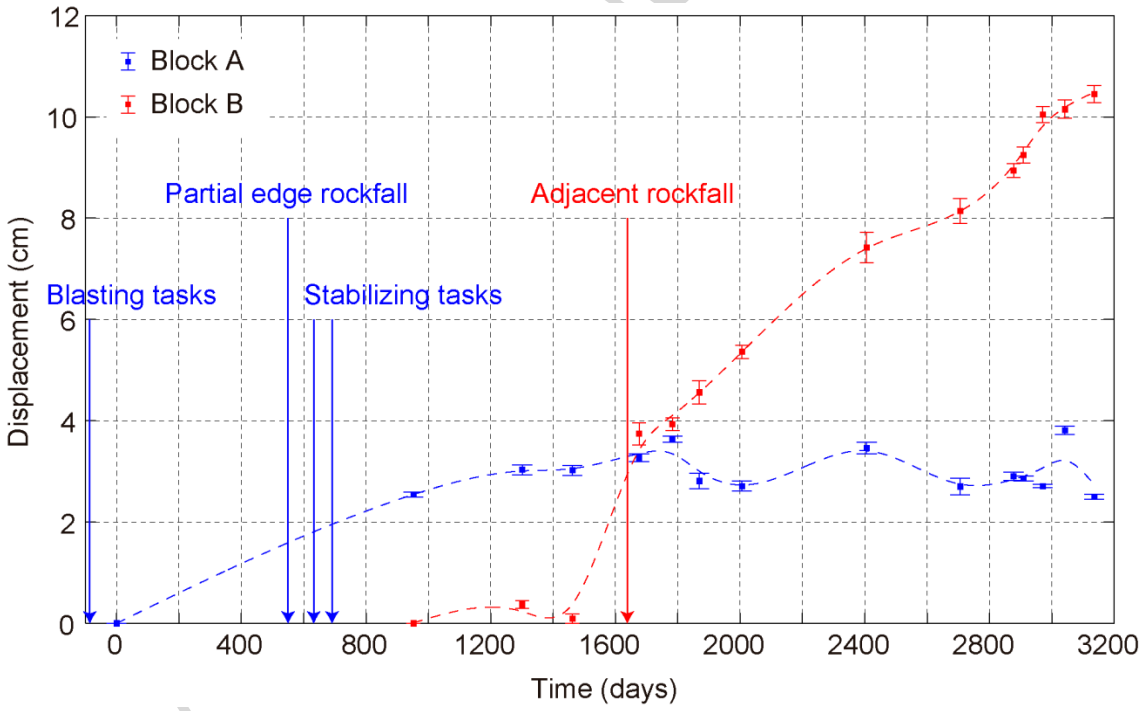

Figure 19. Movement evolution for two blocks in the Degotalls North wall over time measured with TLS. Main facts conditioning their stability are also indicated.

The second instability (Block B, in the figure 18) was detected in the period from May 2011 to December 2011 in a block close to a small rockfall which occurred during the same period (07/11/2011). An initial mean movement of 4 cm was detected and in this case no stabilization works were undertaken because of the small size of the block in relation to the rockfall fences already existing for the road protection, so an increment of the displacement has been recorded (figure 19). Until December 2015 the accumulated displacement in this block was over 10 cm showing the need to continue with the monitoring survey, although the TLS seasonal frequency makes it difficult to use it as a prevention tool. Several surveying prisms for the block A are to be added in late 2016 to contrast the TLS measurements with the Total Station technique (with slightly higher precision). The total amount of displacement that the block is able to accumulate before falling depends on the particular stability conditions of the block; for hard rock massif and isolated rockfall detachment, it is expected to be small [Janeras *et al.* 2010]. Despite the stiffness of the conglomerate rock mass (both intact rock and discontinuities), the observed displacements (figure 19) lead us to question if M1 mechanism

(Table 1) has a brittle behaviour. Nevertheless, the localized rupture in each rock bridge along the joint may be highly brittle. Also, the interleaved softer rocks like siltstone may be conditioning the mechanical behaviour of these discontinuities.

Finally, for the pilot test of GBSAR at the Guilleumes site, the displacement map of the rock cliffs can be constructed using the zero baseline adaptation of the CPT technique [Iglesias *et al.* 2015a]. Figure 20 shows a preliminary result obtained using a daily dataset of 34 SAR images. Non-significant displacements are observed on the surface of the rock cliffs, showing stable behaviour during the measurement campaign.

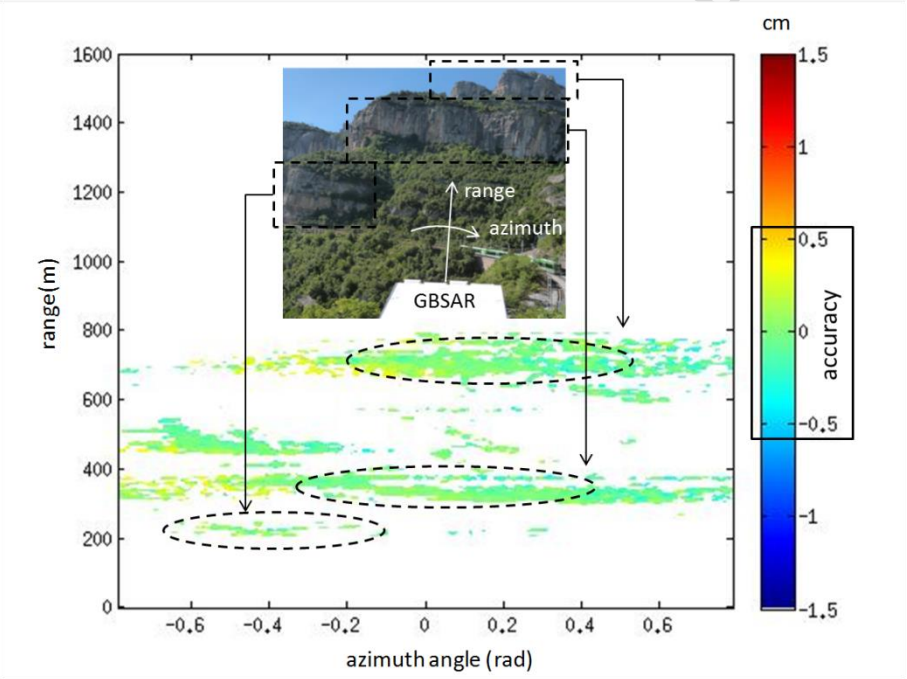

Figure 20. Displacement map (in polar coordinates, every pixel is related to its radar azimuth and range coordinates regarding the SAR location and orientation) retrieved after DInSAR processing at the Guilleumes site. Non-significant displacements have been observed during the 5-month test within the achieved accuracy that doubles the sensibility range of the instrument (±2.5 mm).

3.4. Comparison of the monitoring techniques

The results from the previous sections show that the different monitoring techniques are highly complementary. Each has its own strengths and weaknesses as is shown in table 5. We plan to increase the number of sites where TLS is applied and spread the simple methodology of Total Station to other points around the mountain in order to cross-check it with other techniques. Although further tests are needed for more in-depth exploration of the GBSAR applications, at least we may extract some lessons from the present state of knowledge, facilitating strategy performance in the short term:

- A remote sensing technique (TLS or GBSAR) becomes useful as the size of the monitoring area increases, and it can detect block movements with precursory centimetre-scale displacements, which may occur before failure. On the one hand, TLS has also the capacity to detect small precursory rockfalls; on the other hand, it is expected that GBSAR could improve the accuracy, or enlarge the covered area, despite affecting the pixel size.
- For the blocks where instability is detected or the highest priority set, contact sensor monitoring is needed to achieve the best accuracy, allowing a proper characterization of the rupture mechanism. Depending on the site characteristics in risk terms and strain rate, Total Station can also be an adequate alternative to be considered.

Table 5. Indicative summary of the typical features according to preliminary testing and the ability to detect deformations of the rock mass (in gray scale intensity) in Montserrat for the various techniques applied until now.

Techniques	Typical performances *			Strain measurement capability	
	Target	Accuracy	Maximum distance	Micro-strain (millimetre)	Macro strain (centimetre)
Crackmeters	Point (sensor placement)	0.05 mm	---	Adequate	Adequate (if within sensor's range)
Total Station	Point (prism placement)	Around 0.8 mm	600 m	Limited	Adequate
GBSAR X-band	Raster (pixel larger than 3 m^2)	3 – 5 mm	800 m	Poor	Limited
GBSAR Ku-band	Raster (pixel larger than 0.75 m^2)	<1 mm expected	300 m	(To be checked)	Adequate (if continuous monitoring)
TLS	Raster (pixel around 0.01 m^2)	5 – 10 mm	400 m	Poor	Adequate (confirmed)

* According to specific mountain slope conditions

4. Conclusions

We are on the road to improving our knowledge of the behaviour of the rock mass in Montserrat Mountain and our understanding of the geomechanical processes leading to rockfall failures. One of the main difficulties in reaching this goal is the stiff and apparently brittle behaviour of the rock mass, so it is necessary to achieve the best possible precision in measurements. However, the applied monitoring techniques are providing interesting results. Preliminary observations show movements at two scales:

On the one hand, millimetre scale displacements are registered as a daily/seasonal response to temperature oscillations within a range of up to 2 mm in joints (A3-6 block) and up to 8 mm at the top of certain rock needles (Cadireta). The recorded displacements are largely recoverable, but cumulative drifts are also detected. The elastic component indicates the degree of disconnection or free movement of the block in relation to the rock mass, while its plastic component indicates progress towards instability, although it may be long-term. This level of rock mass strain is currently out of range for the remote sensing methods, and will be analyzed in further detail through the contact sensor instrumentation. In the near future, an in-situ test site will be instrumented with extensometers and thermistor in rock mass depth to see the thermo-mechanical coupling similar to other experiments (Ruiz-Restrepo 2013).

On the other hand, there are centimetre-scale movements in blocks where the rupture mechanism is clearly identifiable and a precarious stability can be assessed. This strain range would be a sign of rupture progression and approach to failure in a shorter term. These deformations are within the range of accuracy of three remote systems, which allows wide spatial coverage campaigns for the detection of a potentially unstable block to be considered in detail.

The different monitoring techniques are providing coherent results, with regard to each time-series length and increasing experience in their application in Montserrat. Taking into account the best aspects of each technique, the results show complementary contributions of the four techniques that should be explored in detail to set up the optimal strategy for the risk mitigation purposes. At the same time, these techniques enable us to accurately quantify the rockfall activity, the TLS being a valuable tool for detecting unnoticed rockfalls. These data are also very useful in assessing the magnitude-frequency relationship for rockfall hazard assessment.

In the future work, we aim to detect precursory signs of rockfall before detachment, either through rock mass strain or precursory small rockfalls. Improved understanding of the mechanical behaviour of the rupture process leading up to rockfall could provide tools for risk management in this area.

Acknowledgments

All these works are supported by the Catalan Government, thanks to the current intervention plan promoted by Patronat de la Muntanya de Montserrat and managed by ICGC. Regarding teamwork, we acknowledge the contribution of the ICGC staff involved from the geological engineering and instrumentation networks departments: Ferran López, Txus Carbonell, Judit Pons, Guillem Domènech, Elisabet Prat, Xavier Rodríguez, Toni Marcè & Àlex Elvira. We also extend the acknowledgement to other contributors at any stage of these works, like Fabian Cabranes from the UPC. We are grateful to A. Abellán for his contribution in the early stage of TLS monitoring, and D. García-Sellés for his technical support in fieldwork campaigns. We also acknowledge the logistic support and predisposition of the security service of the monastery and the Benedictine community.

Authors and their corresponding research groups in each part of the project acknowledge the support of several projects and institutions as follows: the "ROCKRISK" research project (Reference BIA2013-42582-P, Spanish Ministry of Economy and Competitiveness); the equipment lent by Infraestructures.cat (public company for civil works promotion by the Catalan Government); the CHARMA project (Reference CGL2013-40828-R, Spanish Ministry of Economy and Competitiveness); the support for GBSAR operation by the Spanish Ministry of Science and Innovation (MICINN) under project TEC2011-28201-C02-01.

Finally, we sincerely thank editors for the possibility of including our work in this special issue, and we acknowledge both reviewers for their valuable assistance improving the text.

References

Abellán A, Jaboyedoff M, Oppikofer T and Vilaplana JM 2009 Detection of millimetric deformation using a terrestrial laser scanner: experiment and application to a rockfall event *Nat. Hazards Earth Syst. Sci.* **9** 365–72

Alippi, C., Camplani, R., Galperti, C., & Roveri, M. (2008). Effective design of WSNs: From the lab to the real world. *Proceedings of the 3rd International Conference on Sensing Technology, ICST 2008*, 1–9. http://doi.org/10.1109/ICSENST.2008.4757063

Alsaker E, Gabrielsen RH and Roca E 1996 The significance of the fracture patterns of Late-Eocene Montserrat fan-delta, Catalan Coastal Ranges (NE Spain) *Tectonophysics* 266 465–91

Arosio D, Longoni L, Papini M, Scaioni M, Zanzi L and Alba M 2009 Towards rockfall forecasting through observing deformations and listening to microseismic emissions *Nat. Hazards Earth Syst. Sci.* **9** 1119–31

Beutel, J., Buchli, B., Ferrari, F., Keller, M., Zimmerling, M., & Thiele, L. (2011). X-SENSE: Sensing in extreme environments. *Design, Automation Test in Europe Conference Exhibition (DATE), 2011*, 1–6. http://doi.org/10.1109/DATE.2011.5763236

Brodu N and Lague D 2012 3D terrestrial LiDAR data classification of complex natural scenes using a multi-scale dimensionality criterion: Applications in geomorphology *ISPRS J. Photogrammetry and Remote Sensing* **68** 121–34

Cabranes, F 2015 *Estudio geomecánico de la estabilidad de la Cadireta d'Agulles (Montserrat)* (*Unpublished* B.Sc.Degree Thesis, ETSECCPB, Technical University of Catalonia) p 156

Chen Y and Medioni G 1992 Object modelling by registration of multiple range images *Image Vis. Comput.* **10** 145–55

Collins, B. D. & Stock, G. M. 2016. Rockfall triggering by cyclic thermal stressing of exfoliation fractures. *Nature Geoscience*, vol. 9, pp. 395-400

Corominas, J., Iglesias, R., Aguasca, A., Mallorquí, J. J., Fàbregas, X., Planas, X., & Gili, J. A. (2015). Comparing Satellite Based and Ground Based Radar Interferometry and Field Observations at the Canillo Landslide (Pyrenees). In *Engineering Geology for Society and Territory*-Volume 2 (pp. 333-337). Springer International Publishing

Crosta, G. B., di Prisco, C., Frattini, P., Frigerio, G., Castellanza, R. and Agliardi, F. (2014). Chasing a complete understanding of the triggering mechanisms of a large rapidly evolving rockslide, Landslides, 11(5), 747–764

Ester M, Kriegel H, Sander J and Xiaowei Xu X 1996 A density-based algorithm for discovering

clusters in large spatial databases with noise *Proc. 2nd Int. Conf. on Knowledge Discovery and Data Mining*

Fontquerni S, Vilaplana JM, Guinau M, Royán MJ, 2013 El factor exposición en el análisi del riesgo geológico. Aplicación a los desprendimientos de roca en la montaña de Montserrat. *Seguridad y Medio Ambiente*. 131: 8-25

Gabriel AK, Goldstein RM and Zebker HA 1989 Mapping small elevation changes over large areas: Differential radar interferometry *J. Geophys. Res.* vol. 94 **B7** 9183

Gallach X 2012 Estudi de susceptibilitat de caiguda de roques a la paret del Monestir de Montserrat a partir de la inspecció d'indicadors d'inestabilitat i d'anàlisi SIG (*Unpublished* M.Sc.Degree Thesis, UB, University of Barcelona) p 32

Hasler, A., Talzi, I., & Beutel, J. (2008). Wireless sensor networks in permafrost research-concept, requirements, implementation and challenges. *Ninth International Conference on Permafrost*, 669–674. Retrieved from ftp://ftp.tik.ee.ethz.ch/pub/people/beutel/HTBTG2008.pdf

Hencher, S. R., Lee, S. G., Carter, T. G., & Richards, L. R. 2011. Sheeting Joints: Characterisation, Shear Strength and Engineering. *Rock Mechanics and Rock Engineering*, 44 (1), 1–22

Iglesias R, Aguasca A, Fabregas X, Mallorqui JJ, Monells D, López-Martínez C and Pipia L 2015 Ground-Based Polarimetric SAR Interferometry for the Monitoring of Terrain Displacement Phenomena–Part I: Theoretical Description *IEEE Journal of Selected Topics in Applied Earth Observations and Remote Sensing* **8** 980–93

Iglesias R, Aguasca A, Fabregas X, Mallorqui JJ, Monells D, López-Martínez C and Pipia L 2015 Ground-Based Polarimetric SAR Interferometry for the Monitoring of Terrain Displacement Phenomena–Part II: Applications *IEEE Journal of Selected Topics in Applied Earth Observations and Remote Sensing* **8** 994–1007

Iglesias R, Fabregas X, Aguasca A, Mallorqui JJ, López-Martínez C, Gili JA and Corominas J 2014 Atmospheric phase screen compensation in ground-based SAR with a multiple-regression model over mountainous regions *IEEE Trans. Geosci. Remote Sens.* **52** 2436–49

Intrieri E, Gigli G, Mugnai F, Fanti R, Casagli N, 2012. Design and implementation of a landslide early warning system. Engineering Geology 147-148, 124-136

Janeras M, Macau A, Figueras S and Comellas J 2010 Prevention and control of rocky slope instabilities induced by blasting vibration in tunneling – application to Núria rack railway *Rock Mechanics in Civil and Environmental Engineering* (Lausanne: ed J Zhao, V Labiouse, JP Dudt, JF Mathier EUROCK 2010)

Janeras M, Palau J, Prat E and Ripoll J 2011 Montserrat: on a long way to rock fall risk mitigation – First experiences, some lessons and future perspectives *Interdisciplinary Rockfall Workshop* (Innsbruck – Igls: RocExs)

Janeras M, Palau J, Prat E, Pons J, Rodríguez H, Martínez P and Comellas J 2013 Valoración de 10 años de mitigación del riesgo de caída de rocas en el Cremallera de Montserrat *VIII Simposio Nacional sobre Taludes y Laderas Inestables* (Palma de Mallorca: ed E Alonso, J Corominas and M Hürlimann)

Janeras, M., Jara, J. A., López, F., Marturià, J., Royán, M. J., Vilaplana, J. M., Aguasca, A., Fàbregas, X., Cabranes, F., Gili, J. A. (2015). Using several monitoring techniques to measure the rock mass deformation in the Montserrat Massif. In: International Symposium on Geohazards and Geomechanics (ISGG 2015, Warwick) IOP Conf. Series. *Earth and Environmental Science* (Vol. 26, p. 012030). http://doi.org/10.1088/1755-1315/26/1/012030

Kawamura, Y., Moridi, M. A., Sharifzadeh, M., & Jang, H. (2014). Development of Underground Mine Communication and Monitoring Systems by Using ZigBee Technology. In Shimizu, Kaneko, & Kodama (Eds.), *ARMS8 - Rock Mechanics for Global Issues* (pp. 1411–1420). Sapporo.

Kromer, R. A., Hutchinson, D. J., Lato, M. J., Gauthier, D. and Edwards, T. 2015. Identifying Rock Slope Failure Precursors Using LiDAR for Transportation Corridor Hazard Management, Eng. Geol., 195, 93–103

Lato, M. J., Diederichs, M. S., Hutchinson, D. J. & Harrap, R. 2012. Evaluating roadside rockmasses for rockfall hazards using LiDAR data: optimizing data collection and processing protocols. Natural Hazards, 60 (3), 831–864.

López-Blanco, M., Marzo, M., Burbank, D. W., Vergés, J., Roca, E., Anadón, P. & Piña, J. 2000 Tectonic and climatic controls on the development of foreland fan deltas: Montserrat and Sant

Llorenç del Munt systems (Middle Eocene, Ebro Basin, NE Spain) *Sedimentary Geology*, 138 (1-4), 17-39

Massonnet D and Feigl KL 1998 Radar interferometry and its application to changes in the Earth's surface *Rev. Geophys.* vol. 36 **4** 441

Oppikofer, T., 2009. *Detection, analysis and monitoring of slope movements by high-resolution digital elevation models*. PhD in Geology, University of Lausanne, Switzerland

Palau J, Janeras M, Prat E, Pons J, Ripoll J, Martínez P and Comellas J 2011 Preliminary assessment of rockfall risk mitigation in access infrastructures to Montserrat *Second World Landslide Forum* (Rome)

Petrie G and Toth CK 2008 Introduction to laser ranging, profiling and scanning *Topographic Laser Ranging and Scanning: Principles and Processing* ed J Shan and CK Toth (London: CRC Press / Taylor & Francis) pp 1–28

Pipia L, Fabregas X, Aguasca A and Lopez-Martinez C 2008 Atmospheric artifact compensation in ground-based DInSAR applications *IEEE Geosci. Remote Sens. Lett.* **5** 88–92

Royán MJ and Vilaplana JM 2012 Distribución espacio-temporal de los desprendimientos de rocas en la montaña de Montserrat Cuaternario y Geomorfología 26 **1–2** 151–70

Royán MJ, Abellán A, Jaboyedoff M, Vilaplana JM and Calvet J 2014 Spatio-temporal analysis of rockfall pre-failure deformation using Terrestrial LiDAR *Landslides* **11** 697-709

Royán MJ, Abellán A, Vilaplana JM 2015 Progressive failure leading to the 3 December 2013 rockfall at Puigcercós scarp (Catalonia, Spain) *Landslides* DOI 10.1007/s10346-015-0573-6

Royán, M. J. (2015). *Caracterización y predicción de desprendimientos de rocas mediante LiDAR Terrestre*. PhD Thesis, University of Barcelona, November 2015

Royán, M.J., Vilaplana, J.M., Janeras, M. & Abellán A. 2016. Detección e inventario de desprendimientos de rocas mediante el seguimiento con LiDAR Terrestre en la Montaña de Montserrat (Catalunya, España). In: *XIV Reunión Nacional de Geomorfología*. Málaga 2016

Ruiz-Restrepo, D. F. 2013. Thermo-Mechanical analysis of the stability of a rock-cliff under climatic actions. Master Thesis at Technical University of Catalonia (UPC)

Tonini M and Abellán A 2014 Rockfall detection from LiDAR point clouds: a clustering approach using R *J. Spatial Information Sci.* **8** 95–110

Zvelebill, J. and Moser, M. 2001. Monitoring based time-prediction of rock falls: Three casehistories, Phys. Chem. Earth, Part B Hydrol. Ocean. Atmos., 26(2), 159–167

- Testing monitoring techniques: Gb-SAR, TLS or LiDAR, jointmetric WSN, Total Station
- Behind recoverable daily/seasonal displacements, cumulative drifts are detected
- Centimetric displacements of blocks are a sign of rupture progression mechanism
- Monitoring techniques provide coherent results and show excellent complementarity
- TLS also detect unnoticed rockfalls for assessing magnitude-frequency relationship